

Article

Openness as Visualization Technique for Interpretative Mapping of Airborne Lidar Derived Digital Terrain Models

Michael Doneus^{1,2}

¹ Department of Prehistoric and Historical Archaeology, University of Vienna, Franz-Kleingasse 1, A-1190 Vienna, Austria; E-Mail: Michael.Doneus@univie.ac.at; Tel.: +43-1-4277-40486; Fax: +43-1-4277-9404

² LBI for Archaeological Prospection and Virtual Archaeology, Hohe Warte 38, A-1190 Vienna, Austria

Received: 16 October 2013; in revised form: 25 November 2013 / Accepted: 26 November 2013 / Published: 28 November 2013

Abstract: Openness is proposed as a visualization technique for the archaeological interpretation of digital terrain models derived from airborne laser scanning. In contrast to various shading techniques, openness is not subject to directional bias and relief features highlighted by openness do not contain any horizontal displacement. Additionally, it offers a clear distinction between relief features and the surrounding topography, while it highlights both the highest and lowest parts of features. This makes openness an ideal tool for mapping and outlining of archaeological features. A comparison with sky-view factor and local relief model visualizations helps to evaluate advantages and limits of the technique.

Keywords: Lidar; airborne laser scanning; Openness; visualization; local relief model; sky-view factor; digital terrain model

1. Introduction

In archaeological prospection, airborne laser scanning (ALS) is mainly used to obtain information about archaeological sites and environmental structures in relief. For this purpose, high quality digital terrain models (DTM) are derived from ALS data, and are subsequently interpreted. Until now, this has mainly been done based on 2D visualizations created from the respective DTM. Of these, simple shaded relief has long been used as a standard visualization technique. While it is easily perceived and “read”, its major drawback lies in the fact that it has reduced information content [1,2]. As a consequence, the number of publications dealing with the problem of displaying and interpreting

archaeological ALS data is constantly growing. Published techniques include dense contour mapping [3], a simple combination of slope and hillshade ([4]; pp. 66–67), geostatistical filtering [5], local relief model (LRM, [6]), principal component analysis (PCA) based on several shaded reliefs with varying illumination angles [1], and sky-view factor (SVF, [7]).

Recently, a number of publications have attempted to compare these visualization methods. Kokalj *et al.* discuss various techniques, including hillshades and derivatives, techniques of elevation differentiations, LRM, SVF, PCA, and various composites [8]. Keith Challis *et al.* [9] published an assessment of visualization techniques and proposed a “toolbox” for low and high relief landscapes, which includes elevation shading, slope severity, solar insolation models and LRM. Another comparison of these techniques was made by Bennett *et al.* [10]. Testing slope, aspect, PCA, local relief model and sky-view factor, it became clear that no technique was able to visualize all of the known relief features. Therefore, a combination of these techniques is the only way to obtain a maximum amount of information on potential archaeological sites in relief.

This brief overview shows that there is abundant literature on visualizing ALS-derived DTMs. Although most of the abovementioned visualization techniques help the user to perceive archaeological and palaeoenvironmental features, not all of them are helpful when trying to delineate individual structures during interpretative mapping. Distinguishing the borderline between an archaeologically induced micro-topographic variation and its surrounding surface can be quite a challenge. This has already been observed by Rebecca Bennett *et al.* [10], who remarked that, with most of the available techniques, the outline of features will shift in a horizontal direction.

For mapping purposes, visualization techniques that “homogenize” archaeologically induced micro-topographic features and enable them to be clearly distinguished from the surrounding terrain become important. The most prominent methods are SVF (see especially ([8]; p. 110)) and LRM, which have been shown to be among the ‘strongest combination of techniques’ ([10]; p. 47). However, as will be demonstrated below, SVF delineates mainly concave features, while LRM does not provide correct outlines of features in certain situations. The aim of this paper is therefore to propose openness as an additional visualization technique for interpretation of archaeological DTMs. It is not subject to directional bias and is very useful for delineating both convex and concave features. In the following section the basic concept of the technique will be explained. Afterwards, openness will be applied to various case studies and the results discussed. Finally, a comparison with SVF and LRM will show the advantages and disadvantages of each method.

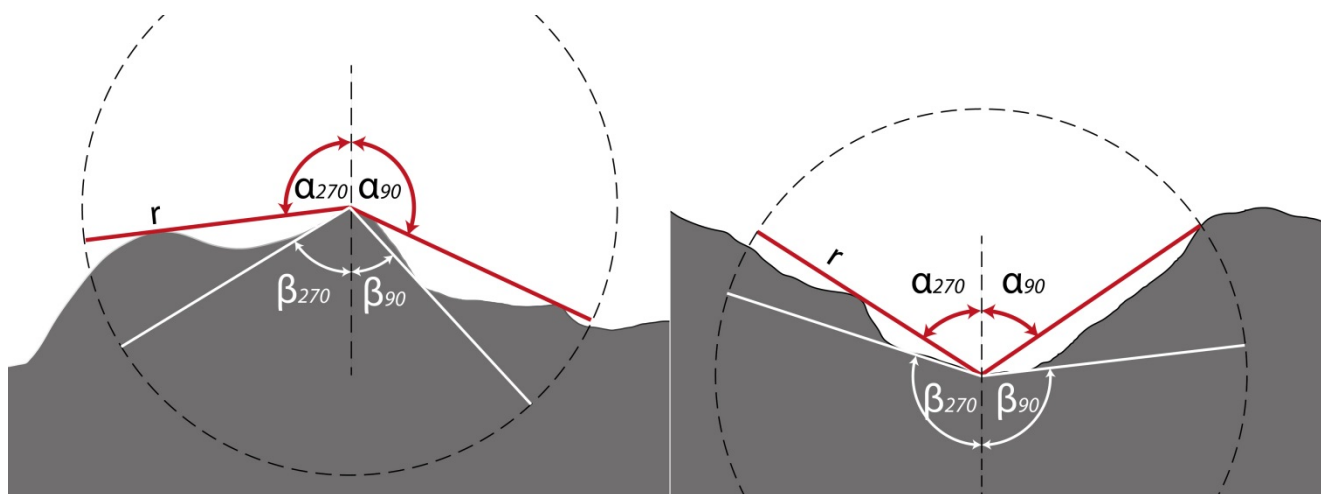
2. The Openness Algorithm

A decade ago, Ryuzo Yokoyama, Michio Shirasawa and Richard J. Pike published “openness” as a then novel way to express ‘the degree of dominance or enclosure of a location on an irregular surface’ ([11]; p. 257). To determine the openness value for a specific location, profiles along at least eight directions (N, NW, W, SW, S, SE, E, NE) are derived from a given digital elevation model within a defined radial distance. Starting from the raster element under consideration, the largest possible zenith (Figure 1, α) or nadir (Figure 1, β) angle along each profile is determined. The mean value of all zenith angles equals the positive openness, while the mean nadir value designates negative openness (Figure 1). The derived values can theoretically range from $>0^\circ$ to $<180^\circ$, where smallest and largest

possible values depend on the cell size of the DTM raster. Perfectly flat surfaces, regardless of whether they are horizontal or tilted, have openness values of 90° .

The chosen radial distance defines a circular kernel or moving window which is moved across the DTM to compute openness for all grid cells. Topographic features outside the kernel will be ignored during calculation of an openness value for the specific location. Therefore, deciding upon the length of the radial distance will have an impact on the calculation results and in consequence on the final visualization. Generally speaking, small distances (a few meters) will enhance local micro-topographic variations, while large values (a few hundred meters) will highlight river valleys and hilltops. Therefore, the size of the radial parameter is directly dependent on the spatial scale of the research question, and this will sometimes necessitate computing openness with different radial parameters.

Figure 1. Calculation of positive (α) and negative (β) openness along two profiles (along East (α_{90} , β_{90}) and West (α_{270} , β_{270}) direction) within a given radial distance (r) in two different topographic situations (after Figure 4 in [11]).



To date, openness has only rarely been used in archaeology. Chiba and Yokoyama combined openness, shaded relief and graduated coloring to generate archaeological maps of artifacts, walls and sites [12]. The author has used positive openness with a radial distance of 1000 m in landscape archaeology to visualize an area of rolling hills and used it as component of a friction surface for least cost path analysis ([13]; p. 311). During this research, tests with different radial sizes were carried out and it was realized that when using small radial values between 5 and 30 m, similar-sized micro-topographic features could be enhanced in a very useful way ([14]; p. 39). Another short mention of openness, which will be discussed below, can be found from Zakšek *et al.* [7].

3. Sample Areas and Processing

In this section, the potential of openness will be demonstrated using various examples taken from two different archaeological ALS missions: (1) a scan of the Leithagebirge in the east of Austria in 2007 [15], and (2) the scan of the archaeological site of Birka-Hovgårdén, located west of Stockholm on the neighboring islands of Björkö and Adelsö, which is one of the case-study areas of the LBI ArchPro [16,17]. The parameters of both scans are listed in Table 1.

Table 1. Parameters of the airborne laser scanning (ALS) data used in this paper.

ALS-Project	Leithagebirge	Birka
Purpose of Scan	Archaeology	Archaeology
Time of Data Acquisition	26 March–12 April 2007	28 and 29 November 2011
Mean Point-Density (last echoes per sq m)	7	11
Strip Overlap	70%	20%
Scanner Type	Riegl LMS-Q560 Full-Waveform	Riegl LMS-Q680i Full-Waveform
Scan Angle (whole FOV)	45°	60°
Flying Height above Ground	600 m	300 m
Speed of Aircraft (TAS)	36 m/s	54 m/s
Laser Pulse Rate	100 000 Hz	400 000 Hz
Scan Rate	66 000 Hz	266 000 Hz
Strip Adjustment	Yes	Yes
Filtering	Robust interpolation (SCOP++)	Robust interpolation (SCOP++)
DTM-Resolution	0.5 m	0.5 m

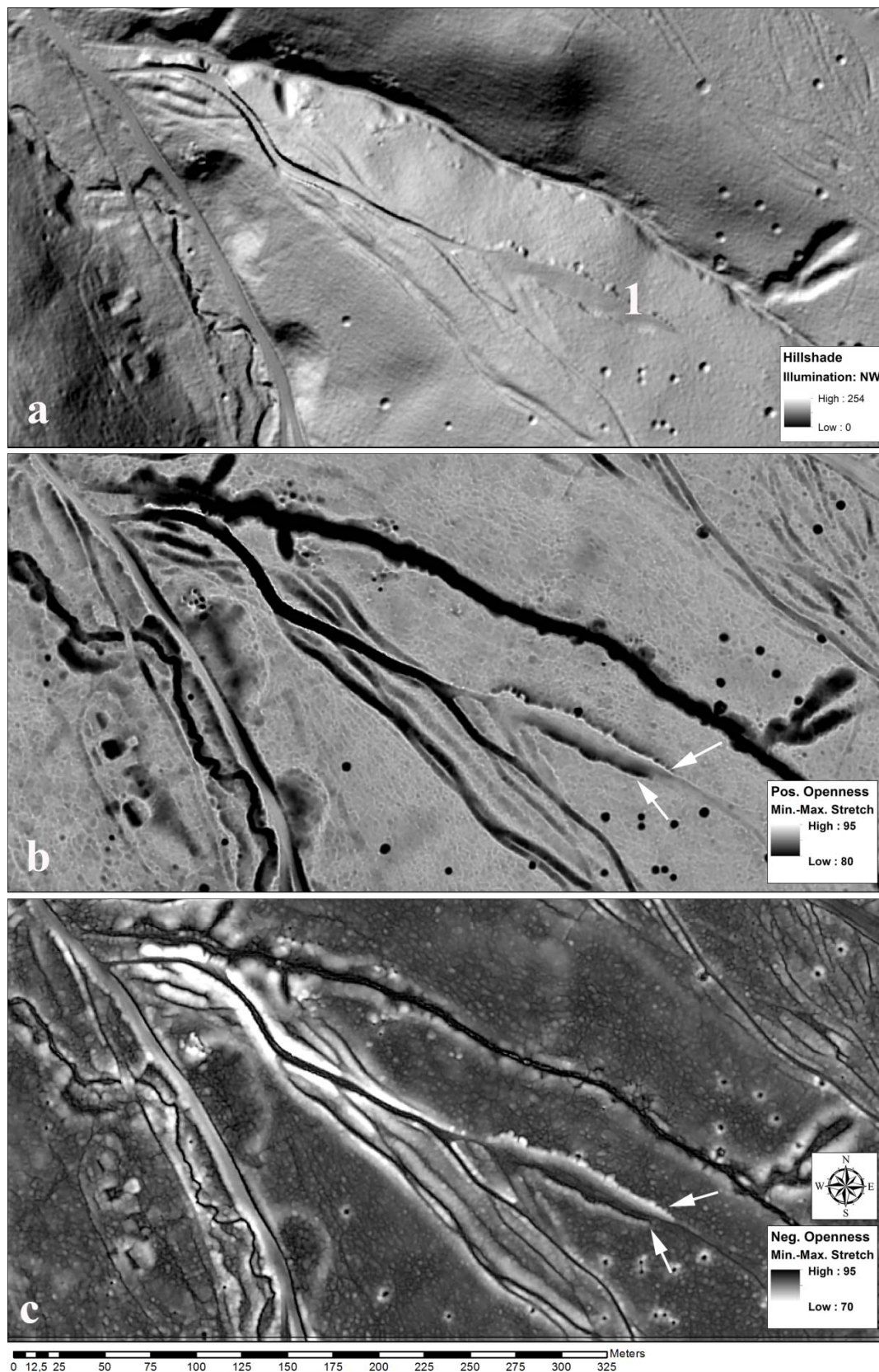
In all cases, openness was calculated using the software package OPALS (Orientation and Processing of Airborne Laser Scanning data), see [18,19]. After testing different kernel sizes, a radial distance with a radius of 15 grid cells (corresponding to 7.5 m) was used for processing. The resulting images display high values as bright and low values as dark tones. Because high positive openness has a different meaning than high negative openness, a simple greyscale coding of both versions would result in an inconsistent symbolization: bright areas denominate crests in positive and valleys in negative openness. To avoid this, the negative openness can be inverted resulting in easier comprehension of the displayed topographic micro-relief. As Kokalj *et al.* [8] have recently suggested for displaying SVF images, a histogram stretch was applied to all openness maps (see image captions for further detail). This resulted in clearly outlined homogenized areas within relief features. Currently, there are also two publicly available tools to calculate openness images, (1) “Relief Visualization Toolbox” from the Institute of Anthropological and Spatial Studies ZRC SAZU [20], and (2) “Lidar Visualization Toolbox” from the Landesamt für Denkmalpflege Baden-Württemberg [21,22].

SVF was calculated using the Relief Visualization Toolbox [20]. LRM models were produced in ArcGIS using a self-developed model, which follows the processing workflow outlined by Hesse [6]. In some cases, openness maps were combined in ArcGIS with other visualization images (e.g., positive and negative openness, positive openness and slope) by setting the top layer to a transparency value of 50%.

4. Result and Discussion

In the following, the effects of positive and negative openness on DTM representation will be demonstrated and discussed. The first example (Figure 2) contains abundant information on modern, archaeological, and natural features. For the sake of this paper, the focus will be set on the hollow-ways of various depths, a terrace (annotation 1 in Figure 2a) and a number of bomb craters from WW2. They are located in the Leithagebirge, east of St Anna in der Wüste (Austria).

Figure 2. Leithagebirge, east of St Anna in der Wüste (Austria). The figure contains hollow-ways of various size and depths, a terrace, and a number of bomb craters from WW2. (a): shaded relief (illumination source in NW), (b): positive openness ($r = 7.5$ m), (c): inverted negative openness ($r = 7.5$ m). All images are histogram stretched.



While the shaded relief visualization (Figure 2a) provides a good impression of the general topography, some of those hollow-ways which run from NW to SE are not clearly visible as they are aligned with the illumination direction (a well-known problem; see [1,2]). In contrast, all linear features are clearly visible in both openness images (Figure 2b,c), which also exclude general topographic information. Neither slopes nor shading are indicated, although the height differences in the map measure 80 m between the upper left and lower right corner of the image. As will be explained below (Section 4.1), this can be regarded as an advantage. Positive openness (Figure 2b), displayed with an applied histogram stretch, depicts the sunken paths and the hollows of the bomb craters in distinct dark tones, which makes them easily identifiable. More importantly, abrupt changes in slope (*i.e.*, at ridges, where up and down slopes intersect or at terraces, where steep slopes change to level surfaces) are outlined as bright lines and can therefore be easily mapped. This is the case at the narrow ridges between the partly intersecting hollow-ways. Also, the rims of the craters are clearly defined. In contrast, features initially seem to be less clear in (inverted) negative openness (Figure 2c). A more thorough investigation, however, reveals additional important information: while the rims are less pronounced at the bomb craters, their deepest parts are now clearly marked by dark spots. Also, the trench bottoms of the individual hollow-ways become distinct as dark lines, rendering the shallow ones clearly visible.

Terrace features also become clearly delineated (annotation 1 in Figure 2a) due to the abrupt change in slope. While the upper edges of terraces display higher (bright) values in positive openness (arrows in Figure 2b), negative openness will result in higher (dark) values only at lower terrace edges (see arrows in Figure 2c). Thus, both upper and lower terrace edges are outlined, while the width of the “lines” corresponds to the degree of sharpness of the edge. Rounded terrace edges will be represented as wider “lines”.

As can be seen at the hollow-ways in Figure 2, openness turned out to be informative where up and down slopes intersect or abruptly change. This is also the case in Birka, where hundreds of round barrows are in close proximity to each other. The heights of the tumuli depicted in Figure 3 range between 0.5 and 2 m. Positive openness (Figure 3b) shows low values (dark) from the base of the mounds to midway upslope, while the top exposes high values (bright). At some of the barrows, small depressions—probably from prior looting—become visible as small, dark, and roundish areas of lower openness values.

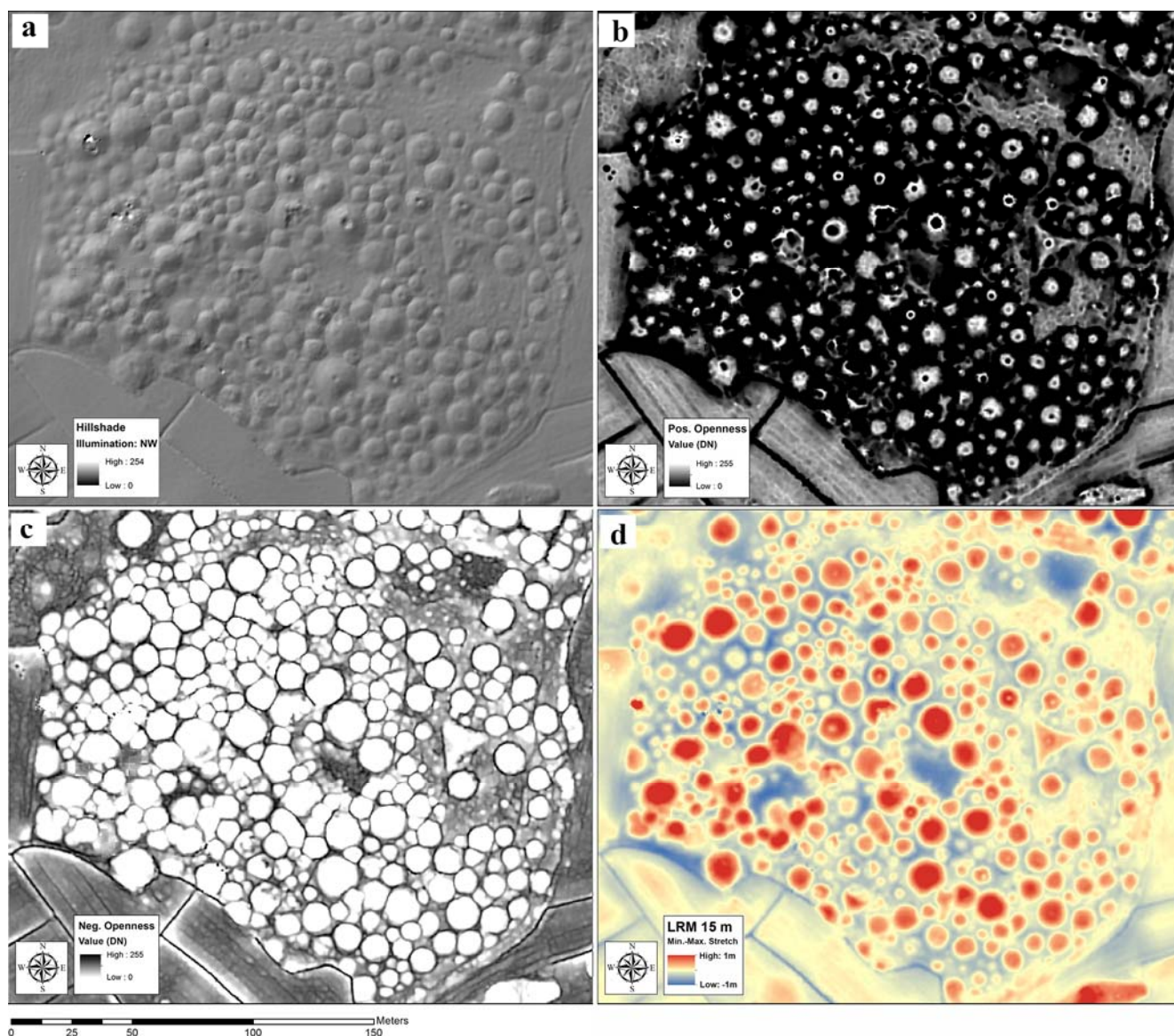
Conversely, inverted negative openness (Figure 3c) clearly delimits all of the barrows through high values at their base (dark), while the mounds themselves have low negative openness values (bright). This visualization is well suited for outlining barrows and similar features during interpretative mapping. The more or less homogenous low openness values (after application of histogram stretching) of the individual barrows also make this visualization suitable for automated classification [23].

Both examples clearly demonstrate the potential of positive and negative openness. In combination, they will both highlight the outlines as well as the highest and lowest parts of sunken and raised relief. What makes this technique so useful for visualization is the fact that openness enhances both local concavities *and* convexities ([11]; p. 257): Openness (in its positive version) quantifies the degree of unobstructedness of a location. Depending on the radial distance, hilltops, peaks and ridges generally will be assigned high values, while valley-bottoms are characterized by low values. Openness is therefore similar to other calculations such as visibility [24], topographic prominence [25], or

sky-view-factor [7]. It is important to stress that as can be seen from Figure 1, negative openness (Figure 1, red lines and α) is not the inverse of positive openness (Figure 1, white lines and β). High negative openness values correspond to valley-bottoms and other low lying structures.

Despite this potential, openness has so far been largely neglected in archaeological literature. Zakšek *et al.* do mention it and compare it with the very similar technique of sky-view factor, but regard it as less ‘intuitive’, because it does not show the general topography ([7]; pp. 403–404). Therefore, openness and SVF need to be compared in order to evaluate their potential in greater detail.

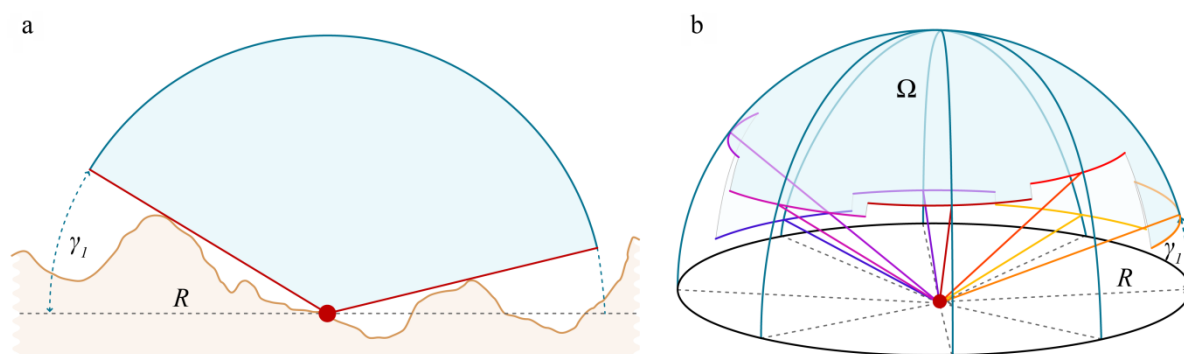
Figure 3. Different visualizations of grave field Hemlanden at Birka (Sweden). (a): shaded relief model (light source in NW); (b): positive openness ($r = 7.5$ m; 2nd standard deviation histogram stretch applied); (c): inverted negative openness ($r = 7.5$ m; 2nd standard deviation histogram stretch applied); (d): local relief model (kernel size = 15 m).



4.1. Openness Compared to Sky-View Factor

As mentioned above, openness is very similar to sky-view factor (Figure 4), which is regarded as highly efficient ([8]; p. 112; [10]; p. 47) and has become an often used visualization technique in archaeological ALS. As its name suggests, SVF quantifies ‘the portion of the sky visible from a certain point’ within a certain radius ([26]; p. 266). Locations with large SVF have a large portion of the sky visible. Similar to openness, the size of the observed area (*i.e.*, the chosen radius) has an effect on the result. To highlight local, small-scale topography, small radii are necessary (e.g., 10–15 m).

Figure 4. Calculation principle of sky-view factor. © Žiga Kokalj and Klemen Zakšek; taken from Figure 2 in [7].



Although openness is similar to SVF, there are three main differences:

(1) Unlike openness, SVF is a physical quantity (the portion of the sky visible indicates also the amount of potential illumination) which can be used in energy balance studies ([7]; p. 403).

(2) SVF uses only zenith angles above the horizontal plane. Therefore, the maximum angle derived during processing SVF can be a zenith of 90° . This means that the SVF (or in other words, the portion of the sky visible from a specific location) cannot be larger than the half-sphere, which would be the case on a perfectly planar, horizontal surface (Figure 4). In contrast, openness also includes angles which are larger. As a result, a location in an openness map will display the same value regardless if it was determined on a tilted or on a horizontal plane, while the sky-view factor of these two locations would differ (Figure 5, see also ([7]; pp. 403–404)). In practical terms, the slope of the general topography will be visible in a SVF image, while it is disregarded in openness. As demonstrated in Figure 6, while the SVF (Figure 6a) also visualizes slope, both positive (Figure 6b) and negative (Figure 6c) versions of openness disregard slope. Although this reduces the “readability” of the general topography ([7]; p. 404), it gives a purer view of the topographic structures, which are no longer masked by slope values. As a consequence, openness values characterizing local micro-topography (e.g., a barrow) will be similar, irrespective of whether the feature is located on a tilted or horizontal plane. This results in more homogeneous “signatures”, which is an advantage for automated classification approaches. If necessary (to enhance the general topographic context), positive openness can be combined with slope. The results of this are very similar to SVF (compare Figure 6a with 6d).

Figure 5. Openness compared to sky-view factor. On a plane surface, both positive (red) and negative (white) openness will result in the same value (90°), regardless of the slope. Sky-view factor (green, hatched line) will differ. On a horizontal plane, it will be larger than on a slope (compare with Figure 1).

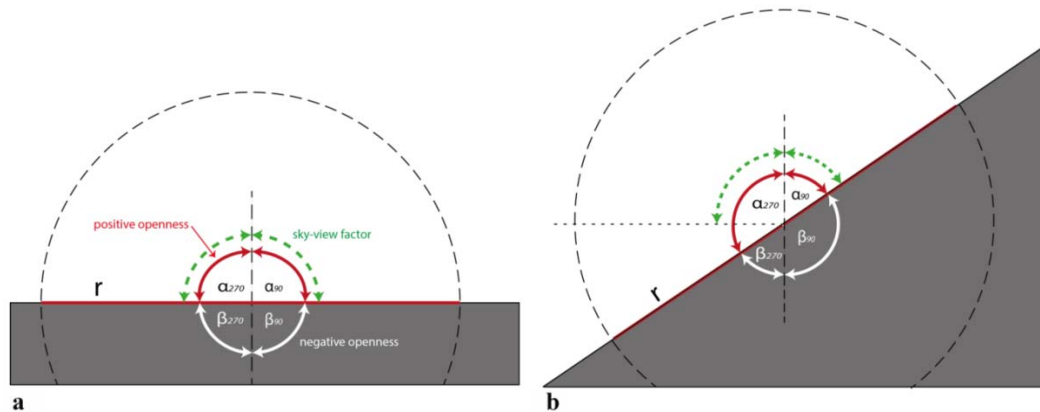
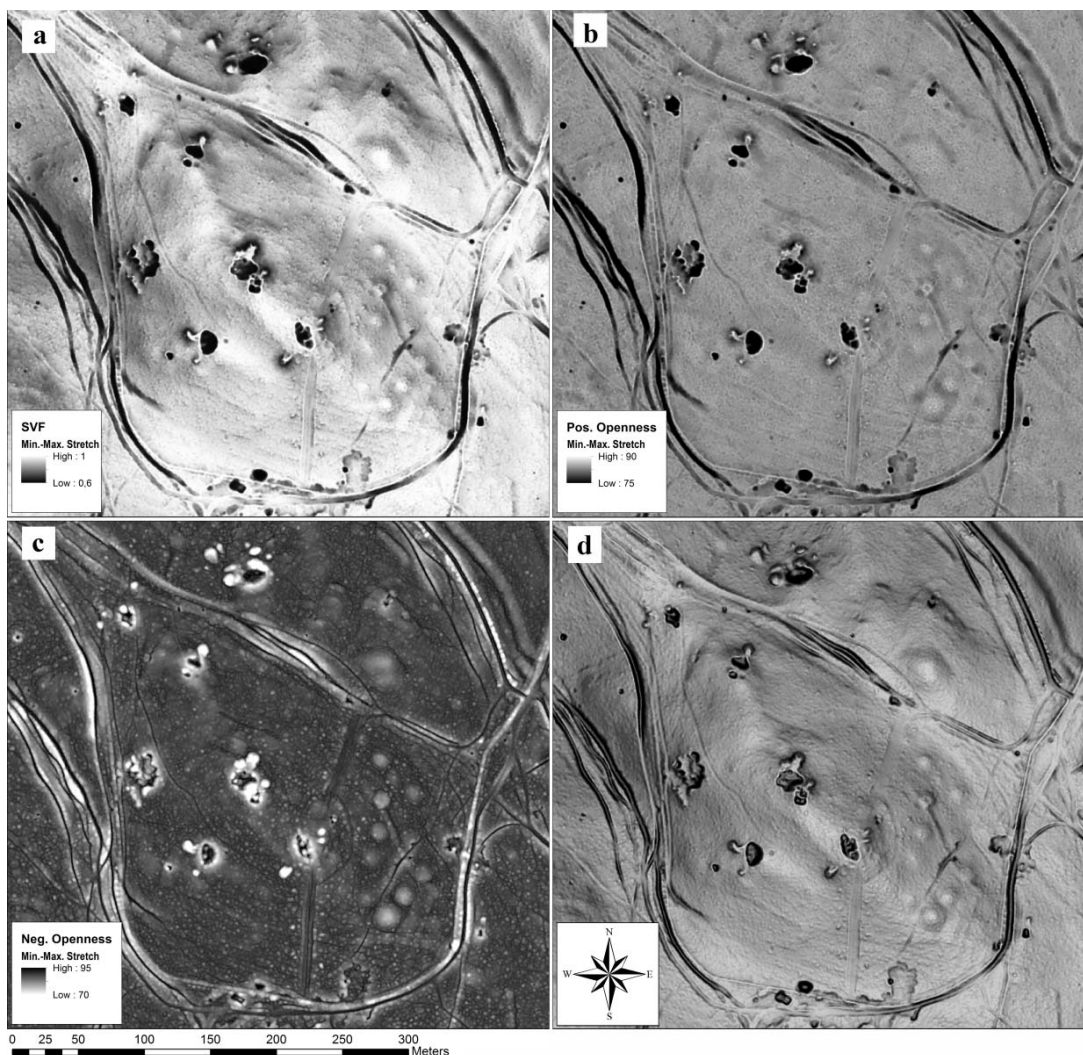


Figure 6. St Anna in der Wüste, Leithagebirge (Austria). While the sky-view factor (SVF) (a) also visualizes slope, both positive (b) and negative (c) versions of openness disregard slope. To enhance the general topographic context, positive openness can be combined with slope (d). Kernel radius for SVF and openness is 7.5 m. All images are histogram stretched.



(3) As mentioned above, SVF uses only zenith angles above the horizontal plane. As a result, it delineates mainly concave features ([8]; p. 110). In contrast, an openness process calculates an additional “negative” version using nadir angles (which theoretically could be also computed for SVF). While positive openness highlights ridges and crests, negative openness will mark the deepest parts. As already demonstrated above, this is very useful during manual mapping and can be also important for automated procedures. Figure 2 depicts hollow-ways and bomb craters. While positive openness outlines the ridges of each individual hollow-way and the rims of the bomb craters, negative openness outlines the lowest parts within each structure. In Birka, positive openness highlights topographic convexities and the tops of the burial mounds. Negative openness emphasizes topographic concavities: the bottoms are highlighted by dark lines and show the boundaries of the barrows in Birka quite clearly (Figure 3).

4.2. Openness Compared to Local Relief Model

As demonstrated, openness shows local micro-topography independent of the general topography. Again, this is similar to local relief model, a technique originally published by Hesse [6] which has proven extremely useful for interpretation of ALS-derived terrain models. The idea behind a LRM is to remove the general topography from a scene by subtracting the low-pass filtered terrain model from the original one in an iterative process. Based on the zero contour of the first subtraction (which marks those lines, where the original DTM and the low-pass filtered DTM intersect), a refined or “purged” general topography model is calculated, which is then subtracted from the original DTM [6]. In that way the terrain is flattened, leaving just the micro-topographical features which can then be enhanced by graduated coloring. The advantage of LRM is thus (1) to acquire a visualization which lets the interpreter immediately perceive and discern sunken from raised features, and (2) the possibility to measure height-differences between individual features and the surrounding area, as well as to calculate volumes of individual structures.

Computation of LRM is not straightforward. During calculation various processing steps have to be applied, where—as with openness—a kernel is used to derive statistical parameters from the original DTM. Depending on the kernel size, the resulting visualizations will differ. Therefore, different topographic settings (relief, size and structure of objects) will need different parameters to compute a LRM.

Additionally, LRM visualizations are not always immediately comprehensible. They can only be interpreted correctly when the computation process is understood and taken into consideration (see also [8]; p. 102). This becomes evident at the situation of a terrace or a road which is cut into a slope (Figure 7). The LRM will display a sequence of positive and negative relief, which could be also “read” as an earthwork showing as a ditch accompanied by two banks (Figure 7b) (see also the evaluation by [6]; p. 71). In this situation, a combination of positive and negative openness gives a more distinct image, where the areas of breaking terrain are displayed as dark and white linear areas (Figure 7d).

Figure 7. Leithagebirge, east of St Anna in der Wüste (Austria). Road cut into a slope. While the situation is evident in the hillshade (a), the local relief model (LRM) (b)—as a result of the computation process—displays an ambiguous sequence of positive and negative relief. This is the result of the computation process, where the large-scale relief (a low-pass filtered and purged digital terrain model (DTM)) is subtracted from the original DTM. In comparison, the hillshade (c) is contrasted with the combined visualization of positive and negative openness (d), which is in this case easier to understand and map. The cross-section (e) displays the original profile (black line) and the low-pass filtered version (red).

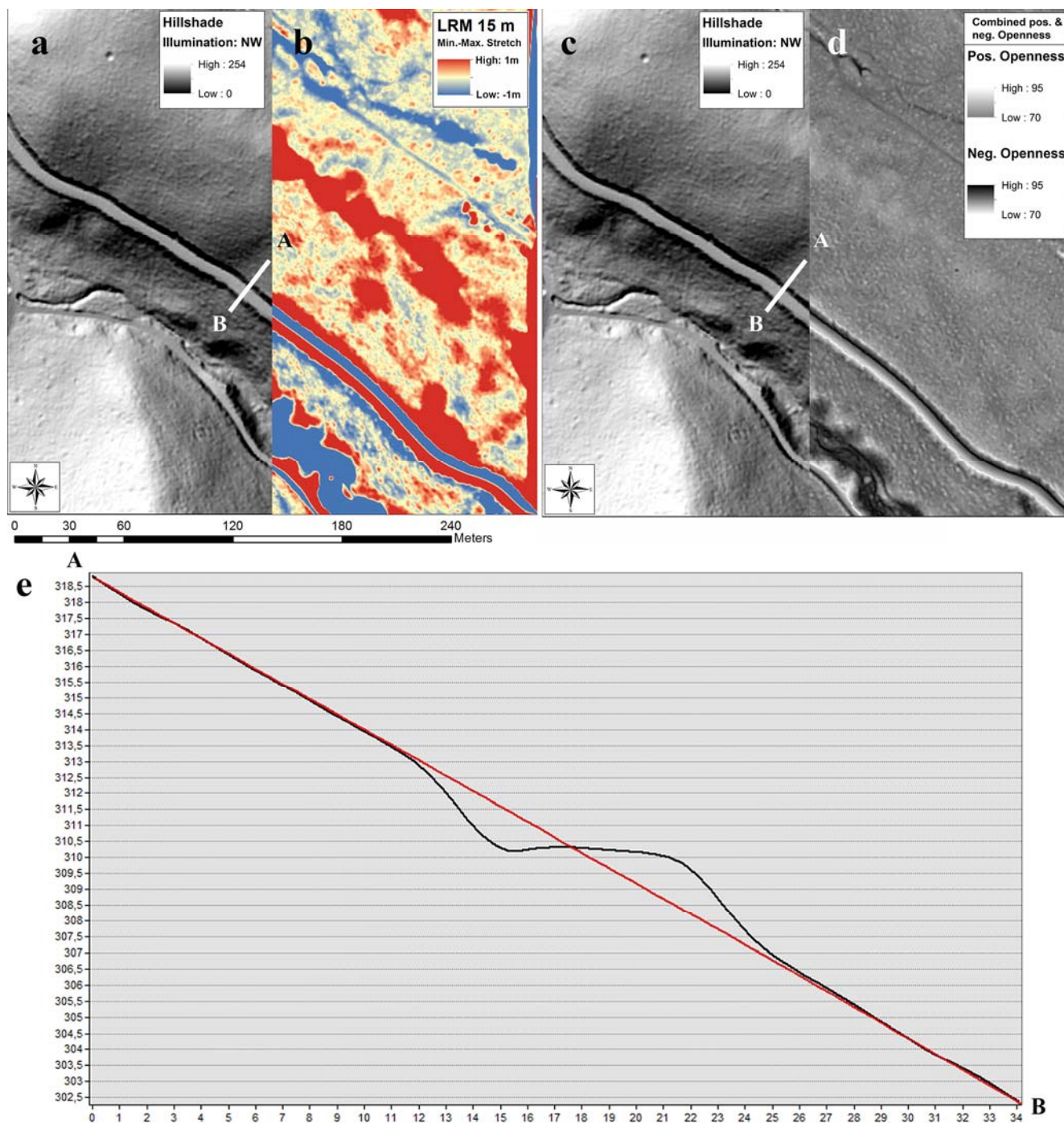


Figure 8. St. Anna in der Wüste (Austria). Detail of Figure 6. Highly eroded round barrows. (a) positive openness; (b) combination of LRM and slope; (c) interpretation.

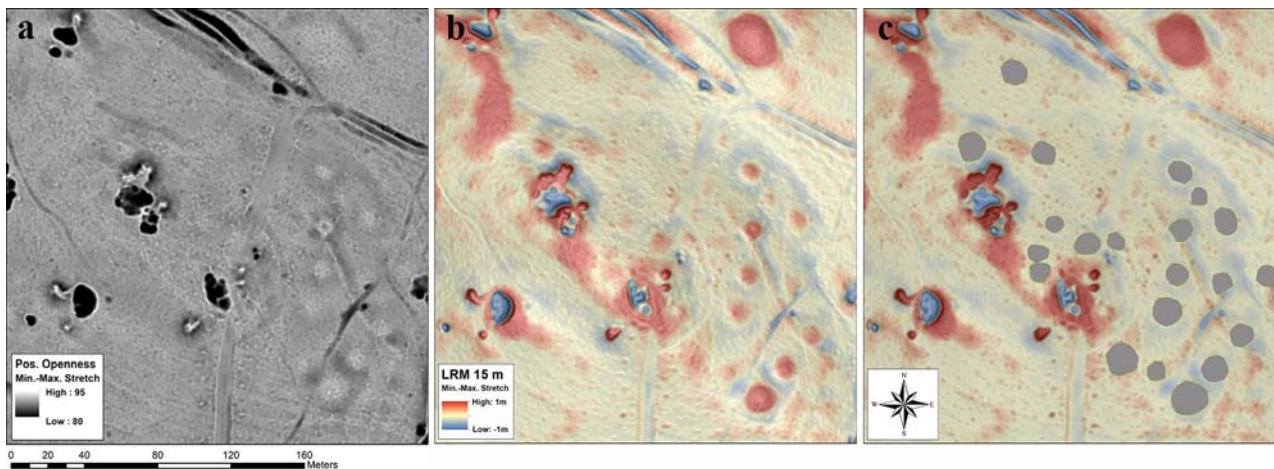
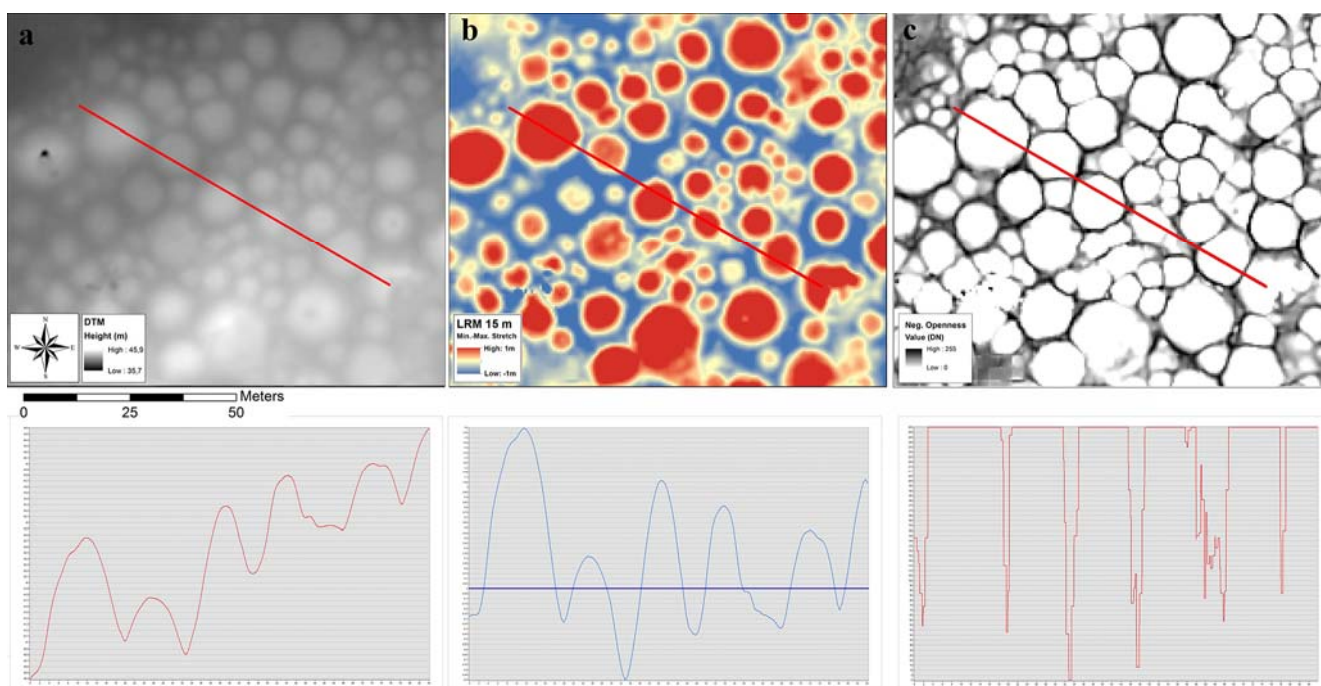


Figure 9. Birka (Sweden)—detail of round barrows. (a) DTM, (b) LRM, (c) inverted negative openness. While the profile of the DTM (a) shows that the round barrows are located on a slope, this general topography is removed due to the process of LRM calculation (b). However, in situations with densely packed upstanding features, the low-pass filter will generate a general terrain which is slightly too high, as indicated by the zero-contour in the profile (blue, horizontal line). This causes the final LRM to incorrectly indicate the extent of each barrow (in red). In comparison, inverted negative openness (c) clearly delineates the individual barrows, thus indicating correct sizes. The profile shows the homogenized values after applying a 2nd standard deviation histogram stretch. Length of all profiles is 84 m. Profile (a) is exaggerated by a factor of 14 (height range 40.4–44.6 m), profile (b) by a factor of 16 (height range –0.9–1.6 m).



In areas of shallow relief, the application of LRM produces clear and distinct visualizations. Figure 8 shows the situation of highly eroded round barrows in the Leithagebirge. While in positive openness (Figure 8a) only nine barrows are visible, according to the interpretation of the LRM the area is covered by at least fifteen burials (Figure 8b,c). This is a clear advantage of LRM over any other known technique and demonstrates the importance of combining various visualizations, since all of them filter and display information content in a different way (see also [9] and [10]; p. 47).

LRM becomes, however, problematic in situations where archaeological topographic features are better preserved (*i.e.*, displaying steeper slopes) and are extremely close to each other, as is the case in Birka. Here, both the low-pass filtered and purged DTM created during the LRM-workflow are slightly too high, resulting in a zero contour which is not at the bottom of the round barrows but cuts through the slope of the barrows (Figure 9b). Therefore, the red areas in the final LRM will not cover the whole barrow, but will be slightly smaller. In comparison, negative openness gives particularly good results in this case. The crests are highlighted by dark lines and show the boundaries of the barrows quite clearly (Figure 9c; see also Figure 3c).

5. Conclusion

This study has examined the use of positive and negative openness to visualize digital terrain models for interpretative mapping of topographic archaeological features. It is the first time that openness has been systematically investigated on a micro-topographic scale using data provided by airborne laser scanning. The examples and comparisons discussed in the paper demonstrate that this technique clearly distinguishes the highest as well as the lowest areas of features such as banks, ditches, and barrows. In contrast to many of the currently available techniques, the highlighted feature extents do not suffer from horizontal shift (as is also true for slope and sky-view factor), which is imperative for accurate interpretative mapping. Thus, openness can be viewed as an important supplementary technique for visualization of archaeological remains present in terrain models derived from airborne laser scanning.

A comparison with the most prominent current archaeological visualization techniques—sky-view factor and local relief model—revealed the advantages and limitations of openness. While local relief models perform better with very shallow relief features, they are problematic in areas with steep relief and large differences in slope, resulting in ambiguously illustrated and incorrectly outlined topographic features. In these situations, openness creates accurate and clear images. In contrast to sky-view factor, openness enhances both convex and concave structures and creates a visualization which is stripped of the general topography, displaying only differences in the micro-relief. Application of a histogram stretch hence results in clearly delineated archaeological features (e.g., bases of barrows, edges of bomb craters, terraces, and hollow-ways).

While openness has been shown to be a valuable technique for the visualization and manual interpretation of archaeological relief features, it could be of even greater use for image analysis applications. The way forward is therefore to investigate the applicability of openness images to function as a basis for (semi-)automatic classification based on pattern recognition and image classification algorithms. This further increases its value as a tool for rapid identification of archaeological features present in large area, high resolution datasets.

Acknowledgements

The Author wants to thank Ralf Hesse, Žiga Kokalj and Geert Verhoeven for their valuable comments and discussion as well as Christopher Sevara for proof-reading the manuscript.

The Ludwig Boltzmann Institute for Archaeological Prospection and Virtual Archaeology (archpro.lbg.ac.at) is based on an international cooperation of the Ludwig Boltzmann Gesellschaft (A), the University of Vienna (A), the Vienna University of Technology (A), the Austrian Central Institute for Meteorology and Geodynamic (A), the office of the provincial government of Lower Austria (A), Airborne Technologies GmbH (A), RGZM-Roman-Germanic Central Museum Mainz (D), RA-Swedish National Heritage Board (S), IBM VISTA-University of Birmingham (GB) and NIKU-Norwegian Institute for Cultural Heritage Research (N).

Conflicts of Interest

The author declares no conflict of interest.

References

1. Devereux, B.J.; Amable, G.S.; Crow, P. Visualisation of LiDAR terrain models for archaeological feature detection. *Antiquity* **2008**, *82*, 470–479.
2. Doneus, M.; Briese, C. Full-Waveform Airborne Laser Scanning as a Tool for Archaeological Reconnaissance. In *From Space to Place: 2. International Conference on Remote Sensing in Archaeology; Proceedings of the 2. International workshop, CNR, Rome, Italy, December 2–4, 2006*; Campana, S., Forte, M., Eds.: Archaeopress: Oxford, UK, 2006; Volume 1568, pp. 99–106.
3. Bewley, R.H.; Crutchley, S.; Shell, C. New light on an ancient landscape: LiDAR survey in the Stonehenge World Heritage Site. *Antiquity* **2005**, *79*, 636–647.
4. Doneus, M.; Briese, C. Airborne Laser Scanning in Forested Areas - Potential and Limitations of an Archaeological Prospection Technique. In *Remote Sensing for Archaeological Heritage Management: Proceedings of the 11th EAC Heritage Management Symposium, Reykjavik, Iceland, 25-27 March 2010*; Cowley, D., Ed.; Archaeolingua; EAC: Budapest, Hungary, 2011; Volume 3, pp. 53–76.
5. Humme, A.; Lindenbergh, R.; Sueur, C. Revealing Celtic Fields from Lidar Data Using Kriging Based Filtering. In Proceedings of the ISPRS Commission V Symposium “Image Engineering and Vision Metrology”, Dresden, Germany, 25–27 September 2006.
6. Hesse, R. LiDAR-derived Local Relief Models—A new tool for archaeological prospection. *Archaeological Prospect.* **2010**, *17*, 67–72.
7. Zakšek, K.; Oštir, K.; Kokalj, Ž. Sky-view factor as a relief visualization technique. *Remote Sens.* **2011**, *3*, 398–415.
8. Kokalj, Ž.; Zakšek, K.; Oštir, K. Visualizations of Lidar Derived Relief Models. In *Interpreting Archaeological Topography: Airborne Laser Scanning, 3D Data and Ground Observation*; Opitz, R.S., Cowley, D., Eds.: Oxbow Books: Oxford, UK, 2013; Volume 5, pp. 100–114.
9. Challis, K.; Forlin, P.; Kincey, M. A generic toolkit for the visualization of archaeological features on airborne LiDAR elevation data. *Archaeol. Prospect.* **2011**, *18*, 279–289.

10. Bennett, R.; Welham, K.; Hill, R.A.; Ford, A. A comparison of visualization techniques for models created from airborne laser scanned data. *Archaeol. Prospect.* **2012**, *19*, 41–48.
11. Yokoyama, R.; Sirasawa, M.; Pike, R.J. Visualizing topography by openness: A new application of image processing to digital elevation models. *Photogramm. Eng. Remote Sens.* **2002**, *68*, 257–265.
12. Chiba, F.; Yokoyama, R. New Method to Generate Excavation Charts by Openness Operators. In Proceedings of the 22nd CIPA Symposium, Kyoto, Japan, 11–15 October 2009; pp. 1–5.
13. Doneus, M. *Die Hinterlassene Landschaft—Prospektion und Interpretation in der Landschaftsarchäologie*; Verl. der Österr. Akad. d. Wiss.: Vienna, Austria, 2013.
14. Doneus, M.; Kühtreiber, T. Landscape, the Individual, and Society: Subjective Expected Utilities in a Monastic Landscape near Mannersdorf am Leithagebirge, Lower Austria. In *Historical Archaeology in Central Europe*; Mehler, N., Ed.: Society for Historical Archaeology: Rockville, MD, USA, 2013; pp. 339–364.
15. Doneus, M.; Briese, C.; Fera, M.; Fornwagner, U.; Griebel, M.; Janner, M.; Zingerle, M.-C. Documentation and Analysis of Archaeological Sites Using Aerial Reconnaissance and Airborne Laser Scanning. In Proceedings of the XXIst International Symposium CIPA: AntiCIPAting the Future of the Cultural Past, Athens, Greece, 1–6 October 2007; Vol. XXXVI-5/C53, pp. 275–280.
16. Trinks, I.; Neubauer, W.; Doneus, M. Prospecting Archaeological Landscapes. In *Progress in Cultural Heritage Preservation: 4th International Conference, EuroMed 2012, Limassol, Cyprus, October 29–November 3, 2012. Proceedings*; Ioannides, M., Fritsch, D., Leissner, J., Davies, R., Remondino, F., Caffo, R., Eds.; Springer: Berlin/Heidelberg, Germany, 2012; Volume 7616, pp. 21–29.
17. Trinks, I.; Neubauer, W.; Nau, E.; Gabler, M.; Wallner, M.; Hinterleitner, A.; Biwall, A.; Doneus, M.; Pregeßbauer, M. Archaeological prospection of the UNESCO World Cultural Heritage Site Birka-Hofgården. In *Archaeological Prospection: Proceedings of the 10th International Conference—Vienna*; Neubauer, W., Trinks, I., Salisbury, R.B., Einwögerer, C., Eds.; Verl. der Österr. Akad. d. Wiss.: Vienna, Austria, 2013; pp. 39–40.
18. Mandlbürger, G.; Hauer, C.; Höfle, B.; Habersack H.; Pfeifer, N. Optimisation of lidar derived terrain models for river flow modelling. *Hydrol. Earth Syst. Sci.* **2009**, *13*, 1453–1466.
19. Mandlbürger, G.; Vetter, M.; Milenkovic, M.; Pfeifer, N. Derivation of a Countrywide River Network Based on Airborne Laser Scanning DEMs—Results of a Pilot Study. In *MODSIM2011, 19th International Congress on Modelling and Simulation. Modelling and Simulation Society of Australia and New Zealand, December 2011*; Chan, F., Marinova, D., Anderssen, R., Eds.; The Modelling and Simulation Society of Australia and New Zealand Inc.: Perth, WA, Australia, 2011; pp. 2423–2429.
20. ZRC SAZU. *Sky-View Factor Based Visualization*; 2013. Available online: <http://iaps.zrc-sazu.si/index.php?q=en/svf> (accessed on 25 November 2013).
21. Hesse, R. Visualisierung hochauflösender digitaler Geländemodelle mit LiVT. *eTopoi Journal of Ancient Studies.* **2013**, in review.
22. LiVT. *Lidar Visualization Toolbox*; 2013. Available online: <http://sourceforge.net/projects/livt/> (accessed on 25 November 2013).

23. Pregesbauer, M. Object *versus* Pixel—Classification Techniques for High Resolution Airborne Remote Sensing Data. In *Archaeological Prospection: Proceedings of the 10th International Conference—Vienna*; Neubauer, W., Trinks, I., Salisbury, R.B., Einwögerer, C., Eds.: Verl. der Österr. Akad. d. Wiss.: Vienna, Austria, 2013; pp. 200–202.
24. van Leusen, M. Visibility and the Landscape: An Exploration of GIS Modelling Techniques? In *[Enter the Past]: The E-Way into the Four Dimensions of Cultural Heritage; CAA 2003; Computer Applications and Quantitative Methods in Archaeology; Proceedings of the 31st Conference, Vienna, Austria, April 2003*; Fischer Ausserer, K., Börner, W., Goriany, M., Karlhuber-Vöckl, L., Eds.: Archaeopress: Oxford, UK, 2004; Volume 1227, pp. 1–15 [CD].
25. Llobera, M. Building Past Landscape Perception with GIS: Understanding Topographic Prominence. *J. Archaeol. Sci.* **2001**, *28*, 1005–1014.
26. Kokalj, Ž.; Zakšek, K.; Oštir, K. Application of sky-view factor for the visualisation of historic landscape features in lidar-derived relief models. *Antiquity* **2011**, *85*, 263–273.

© 2013 by the author; licensee MDPI, Basel, Switzerland. This article is an open access article distributed under the terms and conditions of the Creative Commons Attribution license (<http://creativecommons.org/licenses/by/3.0/>).